Platinum Catalysts Prepared with Functional Carbon Nanotube Defects and Its Improved Catalytic Performance for Methanol Oxidation

Jinhua Chen,* Mingyong Wang, Bo Liu, Zhen Fan, Kunzai Cui, and Yafei Kuang

State Key Laboratory of Chemo/Biosensing and Chemometrics, College of Chemistry and Chemical Engineering, Hunan University, Changsha, 410082, People's Republic of China

Received: February 17, 2006; In Final Form: March 22, 2006

Carbon nanotube (CNT) supported Pt nanoparticle catalysts have been prepared by spontaneous reduction of $PtCl_6^{2-}$ ion as a result of direct redox reactions between $PtCl_6^{2-}$ and oxygen-containing functional groups at defect sites of CNTs, which were introduced by chemical and electrochemical oxidation treatment of CNTs. The electrocatalytic properties of as-prepared Pt-CNT catalysts for methanol oxidation were investigated by chronopotentiometry and cyclic voltammetry. Compared with Pt catalysts prepared by hydrogen reduction and electrochemical deposition methods, Pt catalysts synthesized by functional CNT defects show excellent antipoisoning ability and long-term cycle stability.

Introduction

During the past decade, considerable efforts have been devoted to the development of direct methanol fuel cells (DMFCs) due to its potential application in transport and portable power sources. However, one of the problems is the high anodic overpotential of methanol oxidation due to the poor reaction kinetics,[1] which prevents DMFCs widespread commercial application. It is well-known that platinum is the best single metal catalyst for methanol oxidaiton. But the poor utilization and the poisoning of platinum catalyst by intermediates such as CO_{ads} are the most serious problems. Modification of platinum by a secondary metal such as Ru,[2] Sn,[3] or Co[4] has been widely studied in recent years. The Pt-Ru binary metallic catalyst, when the ratio of Pt:Ru is 50:50, is commonly accepted as the best electrocatalyst for methanol oxidation.[5] Secondary metals were believed to enhance electrocatalytic activity and moderate the poisoning of Pt catalyst by supplying oxygen-containing groups to an adjacent surface site (Pt) at a lower potential than Pt in a so-called bifunctional mechanism.[6]

Carbon nanotubes (CNTs), which have been considered as an attractive support material for noble metal nanoparticles (such as Pt, Pt-Ru, etc.),[7] have perfect structure, but defects arise inevitably during the growth of CNTs[8] and can also be introduced after some postsynthesis treatments such as chemical oxidation by strong acid.[9] In general, the defect sites located at the ends or/and the side walls of CNTs will be preferentially oxidized to oxygen-containing functional groups (such as carboxyl and hydroxyl groups, etc.) because they are more reactive than perfect sites.[10] In previous papers, the high electrocatalytic activities of Pt/CNT and Pt-Ru/CNT electrodes for methanol oxidation are contributed to high dispersion of Pt or Pt-Ru nanoparticles with small particle size due to good electric conductivity and high surface area of CNTs.[11] To our knowledge, no works focus on the possible effects of functionalized CNT defects on the preparation and catalytic activity of Pt catalyst for methanol oxidation. In this paper, we try to demonstrate the possibility that the oxygen-containing functional groups located on the defects of CNTs improve the electrocatalytic properties of Pt catalyst and play a similar function with the secondary catalysts, such as Ru.

On the other hand, previous approaches to attaching metal nanoparticles on CNTs include physical evaporation,[12] electrochemical deposition,[13] solid-state reaction with metal salts at elevated temperatures,[14] grafting after functionalization of CNTs,[15] and electroless deposition from salt solutions with the aid of reducing agents or catalyst.[16]

In this paper, we demonstrate spontaneous reduction of platinum nanoparticles on the surface of multiwalled CNTs (MWNTs) from H_2PtCl_6 aqueous solution without any reductant as a result of direct redox reactions between the metal ion and functional defects of CNTs. This work is motivated by a recent observation by Dai et al. of spontaneous deposition of Pt and Au on sidewalls of single-walled CNTs from Na_2PtCl_4 and $HAuCl_4$ in ethanol solution, respectively.[17] In this way, most of Pt nanoparticles should be deposited on the functional defect sites of MWNTs, which may cause Pt nanoparticles to be surrounded by lots of oxygen-containing functional groups. Compared with Pt and Pt-Ru catalysts prepared by electrochemical deposition or hydrogen reduction methods, Pt catalysts synthesized by functional CNT defects show excellent antipoisoning ability and long-term cyclic stability.

Experimental Section

CNTs used were grown directly on a graphite substrate (1.2 cm in length, 0.6 cm in width, 0.4 cm in height) by a chemical vapor deposition method as reported in a previous paper.[18] The functionalization of CNT defects was carried out by a simple process: The pristine CNTs were oxidized chemically in 5.0 M HNO_3 aqueous solution for 10 h and then cycled in the range of −0.15 to 1.3 V with a sweep rate of 50 mV s^{-1} in 0.1 M H_2SO_4 aqueous solution by cyclic voltammetry (CV) until steady curves were obtained. The oxygen-containing groups on the CNT surface were confirmed by CV and FTIR investigation (WQF-410 spectrometer, Beijing, China).

The preparation procedures of three kinds of catalysts are as follows:

* Corresponding author. Tel/Fax: 86-731-8821848. E-mail: chenjinhua@hnu.cn.

10.1021/jp061045a CCC: $33.50
Published on Web 05/28/2006

(1) Catalyst SR-Pt was synthesized by a spontaneous reduction method. The functional CNT electrode was immersed into 1.3 mM H_2PtCl_6 aqueous solution at 348 K for 15 min. Pt nanoparticles were spontaneously formed on the sidewalls of MWNTs.

(2) Catalysts E-Pt and E-PtRu were prepared by an electrochemical deposition method. Pt and Pt-Ru nanoparticles were electrodeposited on CNT electrodes by potential-step deposition method from N_2 saturated 1.3 mM H_2PtCl_6 and 1.3 mM H_2PtCl_6 + 1.3 mM $RuCl_3$ aqueous solutions, respectively. The potential jumped from 0.2 to −0.25 V (SCE) with a pulse width 0.001 s. The deposition charges are 52.2 and 151.9 μC cm^{-2} for catalyst E-Pt and E-PtRu, respectively. The particle size of catalyst E-Pt (or catalyst E-PtRu) is 50−70 nm.

(3) Catalysts H_2-Pt and H_2-PtRu were obtained by hydrogen the reduction method. Forty microliters of 1.3 mM H_2PtCl_6 (or 1.3 mM H_2PtCl_6 + 1.3 mM $RuCl_3$) aqueous solution was added to the surface of a CNT electrode by a microsyringe. After being allowed to dry in air at room temperature (298 K), the electrode was heated at 673 K under nitrogen−hydrogen atmosphere with a total flow rate of 120 cm^3 min^{-1} (the volume ratio of nitrogen to hydrogen is 100:20) at a pressure of 5.0 Torr for 2 h. The particle size of catalyst H_2-Pt (or catalyst H_2-PtRu) is about 10 nm.

After preparation, all catalysts were rinsed with double-distilled water. The morphology of the catalysts was characterized by scan electron microscopy (JEOL, JSM 5600LV, operating at 20 kV).

The electrochemical performance of catalysts was investigated in 0.1 M H_2SO_4 aqueous solutions with 1.0 M CH_3OH by CV, which was carried out on a CHI 660A electrochemical working station (CH Instrument, Inc.). The CNT electrode with an apparent surface area of 0.72 cm^2 was used as a working electrode. Platinum foil served as a counter electrode, and a saturated calomel electrode (SCE) was used as a reference electrode. All chemicals used were of analytical grade. Fresh double-distilled water was used throughout. All experiments were carried out at 298 K.

Results and Discussion

Thermodynamics of Spontaneous Reduction of $PtCl_6^{2-}$ Ion and the Preparation of Catalyst SR-Pt. The spontaneous deposition of metal nanoparticles on CNTs is ascribed to the redox reaction between carbon nanotubes and metal ion.[17] The driving force for Pt deposition on CNTs could be the difference between the potential of $[PtCl_6]^{2-}$ reduction and the potential of CNT oxidation

$$\Delta E = E_{Pt/PtCl_6^{2-}} - E_{Reduced-CNT/Oxidized-CNT} > 0 \qquad (1)$$

Here $E_{Pt/PtCl_6^{2-}}$ stands for the equilibrium potential of reaction defined by[19]

$$[PtCl_6]^{2-} + 4e^- = Pt^0 + 6Cl^- \qquad (2)$$

$$E_{Pt/PtCl_6^{2-}}(\text{vs SCE}) \approx 0.72 + 0.015 \log[PtCl_6]^{2-}$$

In this paper, $[PtCl_6]^{2-}$ is 1.3 mM, it can be calculated that $E_{Pt/PtCl_6^{2-}}$ is 0.68 V.

On the other hand, Figure 1A shows the redox behavior of functional CNTs. A pair of broad redox peaks (curves a and a′), which correlate with the redox of surface-oxygen-containing groups (such as carboxyl, carbonyl, and hydroxyl groups)[20] on functional CNT defect sites, appears at 0.34 and 0.28 V. The

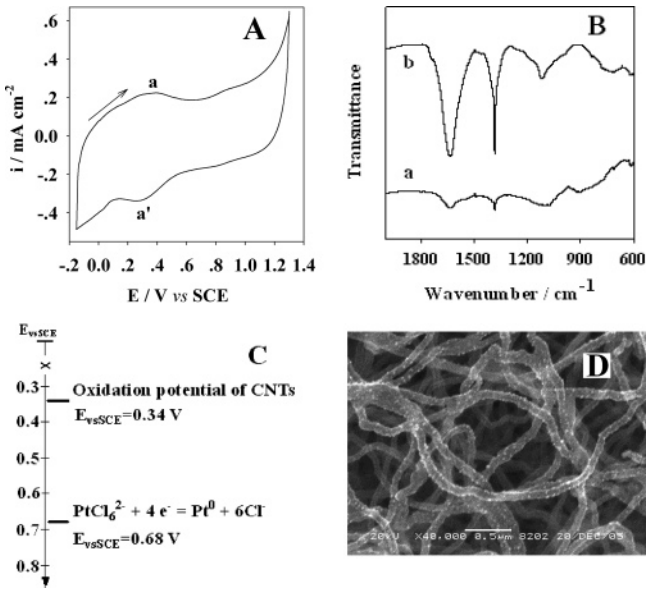

Figure 1. (A) Cyclic voltammograms of the CNT electrode in 0.1 M H_2SO_4 aqueous solution. (B) FTIR spectra of CNTs without (a) and with (b) functional treatments. (C) Diagram showing the oxidation potential of CNTs and the equilibrium potential of $PtCl_6^{2-}$. (D) SEM image of Pt nanoparticles spontaneously formed on CNTs after immersion in $PtCl_6^{2-}$ aqueous solution.

oxygen-containing groups on the CNT surface were also confirmed by FTIR (Figure 1B). For the functional CNTs, two peaks can be observed obviously at 1101 and 1634 cm^{-1}, which are assigned to ν_{C-O} and the carbonyl group, respectively (Figure 1B, curve b). These two peaks for CNTs can also be seen without any treatment (Figure 1B, curve a), but the strength is very weak, which may result from the oxidation of some CNT defects by oxygen in air.

According to Figure 1C, the oxidation potential of the functional CNTs is more negative than the equilibrium potential of the $PtCl_6^{2-}$ ion. This implies that the condition for Pt spontaneous deposition on CNTs defined by eq 1 is satisfied and a familiar galvanic cell between functional CNT defects and $PtCl_6^{2-}$ ion exists. The relative potential levels rationalize the spontaneous electron transfer from the nanotube defects (oxidation) to the metal ions (reduction). The scanning electron microscopy (SEM) image shown in Figure 1D confirms the formation of Pt nanoparticles on CNTs and the diameter of Pt nanoparticles is 10−20 nm.

Cyclic Voltammograms of Methanol Oxidation on Catalyst SR−Pt. The electrocatalytic property of catalyst SR-Pt was investigated by cyclic voltammetry and the corresponding result is shown in Figure 2. Typical feature of methanol oxidation, which is accordant with other works,[8] is observed (Figure 2, curve 1). Two oxidation peaks, which are related to the oxidation of methanol and intermediates, appear at 0.67 and 0.49 V, respectively. To clarify the role of the functional defects of CNTs, a control experiment was carried out on the pristine CNTs without chemical and electrochemical treatments. From curve 2 in Figure 2, no obvious peaks of methanol oxidation can be observed. This implies little Pt catalyst exists on the CNTs and indicates further that the functionalization of CNT defects is an important condition for the spontaneous deposition of Pt on CNTs.

The Chronopotentiometric Curves of Electrocatalysts. Chronopotentiometry is a useful approach to study the anti-poisoning abilities of catalysts for methanol oxidation.[21] Catalyst SR-Pt was characterized by chronopotentiometry and compared

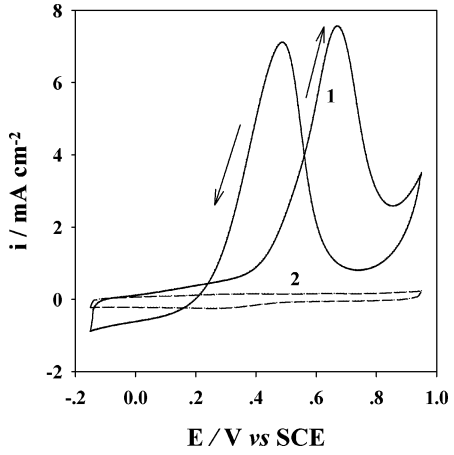

Figure 2. Cyclic voltammogram of catalyst SR-Pt supported on CNTs with (line 1) and without (line 2) functional treatments in 0.1 M H_2SO_4 aqueous solution with 1 M CH_3OH.

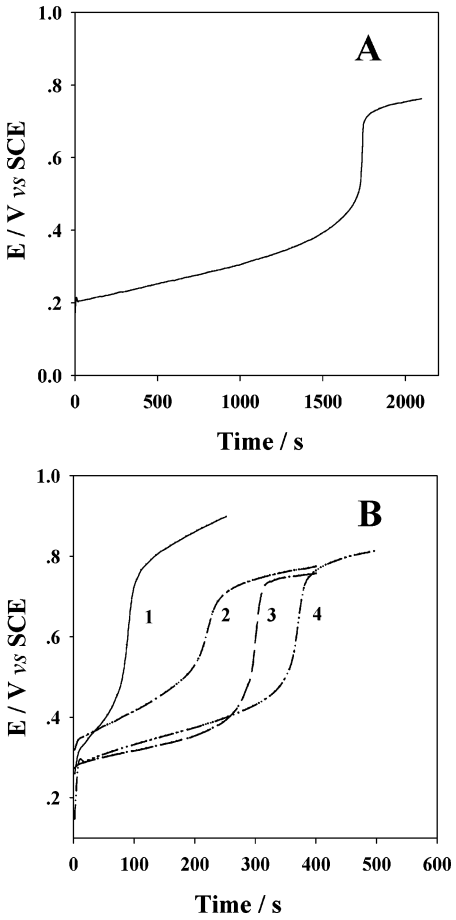

Figure 3. Chronopotentiometric curves of different catalysts in 0.1 M H_2SO_4 aqueous solutions with 1 M CH_3OH: (A) catalyst SR-Pt; (B) catalyst E-Pt (curve 1), catalyst H_2−Pt (curve 2), catalyst E-PtRu (curve 3), and catalyst H_2-PtRu (curve 4).

with other Pt and Pt-Ru catalysts prepared by electrochemical deposition and hydrogen reduction methods. To diminish the influence of the loading mass and electrocatalytic activity of catalyst to the utmost extent, the value of the applied anodic current density is the same as that of the current density at 0.4 V on the forward branch in the corresponding cyclic voltammograms. For all catalysts, it can be seen from Figure 3 that the electrode potential increases gradually for several hundred seconds and then jumps to a higher potential. The reason is as follows: During the chronopotentiometric experiment, the poisonous species, mainly CO_{ads} brought from methanol oxidation, are accumulated on the surface of electrocatalysts and reduce the electrocatalytic activity of catalysts. The potential must be increased to satisfy the applied anodic current density. When the electrocatalysts are poisoned deeply, the methanol oxidation reaction cannot continue. To satisfy the applied anodic current density, the potential must jump to a higher potential, at which H_2O is decomposed.[21]

TABLE 1: The Data of the Onset Potential for Methanol Oxidation and Time (*T*) for Potential Jump Obtained from Figure 3[a]

catalysts	E-Pt	E-PtRu	H_2-Pt	H_2-PtRu	SR-Pt
applied anodic current density (mA cm^{-2})	0.14	0.46	0.09	0.42	0.90
onset potential (V)	0.32	0.28	0.35	0.28	0.21
T (s)	80	290	220	370	1720

[a] The value of the applied anodic current density is the same as that of the current density at 0.4 V on the forward branch in the corresponding cycle voltammograms.

Here, the time (*T*) at which the electrode potential jumps to a higher potential is introduced to judge the antipoisoning ability of catalyst and the corresponding data obtained from Figure 3 are summarized in Table 1. From Table 1, the order of *T* values is as follows: catalyst SR−Pt (1720 s) ≫ catalyst H_2-PtRu (370 s) > catalyst E-PtRu (290 s) > catalyst H_2-Pt (220 s) > catalyst E-Pt (80 s). Also, the onset potential values for methanol oxidation at different catalysts are listed in Table 1 and the following order is observed: catalyst SR-Pt (0.21 V) < catalyst H_2-PtRu (0.28 V) = catalyst E-PtRu (0.28 V) < catalyst E-Pt (0.32 V) < catalyst H_2-Pt (0.35 V). These results show that catalyst SR-Pt has the best electrocatalytic property and antipoisoning ability of these Pt and Pt-Ru catalysts.

Long-Term Cycle Stability of Catalyst SR-Pt. Long-term cycle stability of electrocatalysts for methanol oxidation is another important parameter in practical application of DMFCs. The long-term cycle stabilities of different catalysts prepared in this paper were investigated in 0.1 M H_2SO_4 + 1.0 M CH_3OH aqueous solutions, and the corresponding results are shown in Figure 4A and Table 2. For all catalysts, the peak current density (*i*) obtained from the forward CV scan decreases slowly with the successive CV scans (Figure 4A). For catalyst SR-Pt, the value of peak current density at the 500th scan (i_{500}) remains 95.2% of that at the first cycle (i_1). However, the values of i_{500}/i_1 are only 58.4%, 72.1%, 66.3%, and 80.6% for catalysts E-Pt, E-PtRu, H_2-Pt, and H_2-PtRu, respectively. Also, the recovery abilities of the catalysts (i_f/i_1) were investigated in fresh 0.1 M H_2SO_4 + 1.0 M CH_3OH aqueous solutions after 500 continuous cycles, and the corresponding results are shown in Figure 4B and Table 3. Catalyst SR-Pt shows the best recovery ability, and the values of i_f/i_1 are 97.7%.

The long-term cycle stabilities and recovery abilities of the catalysts were also investigated in 0.1 M H_2SO_4 aqueous solutions with high methanol concentration (2.0 and 4.0 M methanol). Similar results can be observed.

The Possible Mechanism of Catalyst SR-Pt for Methanol Oxidation. On the basis of the above experimental results, an exciting phenomenon is observed: Catalyst SR-Pt has the better antipoisoning ability and long-term cycle stability than Pt and Pt-Ru catalysts prepared by electrochemical deposition and hydrogen reduction methods. This may be exciting for the commercialization of DMFCs. Scheme 1 depicts the procedure of the Pt deposition on CNTs and explains the excellent performance of catalyst SR-Pt for methanol oxidation. The CNTs with defects (step A) were functionalized by 5.0 M nitric

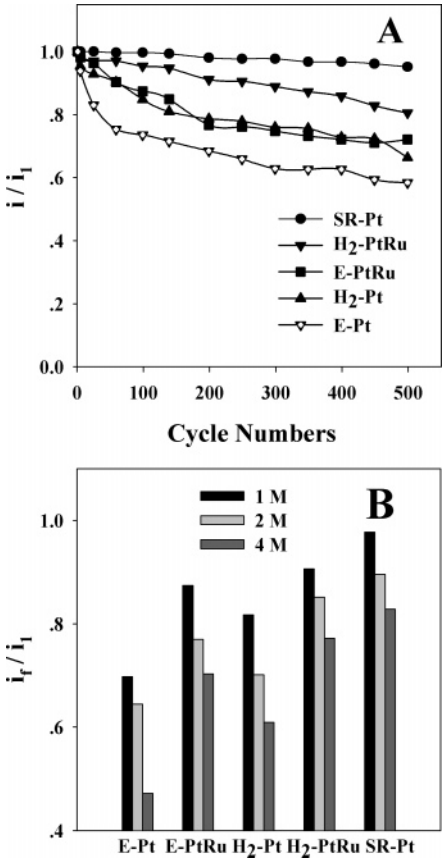

Figure 4. (A) Long-term cycle stabilities of various catalysts in 0.1 M H_2SO_4 aqueous solutions with 1 M CH_3OH. (B) After 500 continuous cycles in 0.1 M H_2SO_4 aqueous solutions with 1, 2, and 4 M CH_3OH, the recovery abilities (i_f/i_1) of the various catalysts in fresh 0.1 M H_2SO_4 aqueous solutions with the same CH_3OH concentration. Here, i_f is the peak current density obtained from the forward CV scan in fresh H_2SO_4 aqueous solutions with the same methanol concentration.

TABLE 2: The Long-Term Cycle Stabilities (i_{500}/i_1) of the Pt and PtRu Catalysts Prepared by Different Methods[a]

methanol concn (M)	E-Pt	E-PtRu	H_2-Pt	H_2-PtRu	SR-Pt
1.0	58.4%	72.1%	66.3%	80.6%	95.2%
2.0	46.6%	67.0%	61.2%	72.3%	76.6%
4.0	39.6%	42.5%	54.4%	53.7%	69.3%

[a] i_1 and i_{500} are the values of the peak current density obtained from the forward CV scan at the 1st and 500th cycles, respectively.

TABLE 3: The Recovery Abilities (i_f/i_1) of the Pt and PtRu Catalysts Prepared by Different Methods[a]

methanol concn (M)	E-Pt	E-PtRu	H_2-Pt	H_2-PtRu	SR-Pt
1.0	69.8%	87.4%	81.7%	90.58%	97.7%
2.0	64.4%	77.0%	77.1%	85.2%	89.5%
4.0	47.2%	70.3%	60.9%	77.2%	82.8%

[a] i_{500} is the value of the peak current density obtained from the forward CV scan at the 500th cycle. i_f is the value of the peak current density obtained from the forward CV scan in fresh solution after 500 continuous cycles.

acid and activated in 0.1 M H_2SO_4 aqueous solution by cycle voltammetry. This procedure not only removes the iron catalyst, which drove CNT growth, but also introduces oxygen-containing groups (such as carboxylic acid, carbonyl and hydroxyl, etc.) at the defect sites of CNTs (step B).[22] When the functional CNTs were immersed in 1.3 mM H_2PtCl_6 aqueous solution, spontaneous reduction of $PtCl_6^{2-}$ would occur at the functional CNT

SCHEME 1: Schematic Illustration of the Basic Methodology for Preparation of Pt Nanoparticles on CNTs

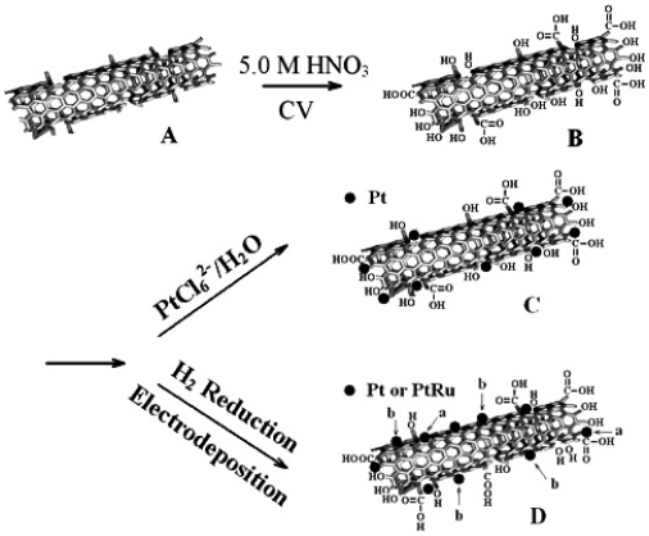

defect sites due to the galvanic cell effect between $PtCl_6^{2-}$ and functional CNT defects (step C). Pt nanoparticles are surrounded by the adjacent oxygen-containing groups such as carboxylic acid and hydroxyl groups. A possible bifunctional effect between Pt nanoparticles and functional CNT defects, which is similar with the well-known bifunctional mechanism between Pt and Ru,[6] occurs during methanol electro-oxidation. In other words, Pt is responsible for catalyzing the dehydrogenation of methanol, while functional CNT defects provide the oxygen-containing groups:

$$5Pt + CH_3OH \rightarrow Pt{-}CO_{ads} + 4Pt{-}H \quad (3)$$

$$CNT + Pt + H_2O \xrightarrow{CV} CNT{-}OH + Pt{-}H \quad (4)$$

$$5Pt{-}H \rightarrow 5Pt + 5H^+ + 5e^- \quad (5)$$

$$CNT{-}OH + Pt{-}CO_{ads} \rightarrow CNT + Pt + CO_2 + H^+ + e^- \quad (6)$$

CNT defects have high reactivity and are easier to be oxidized to oxygen-containing groups at low potential. During CV, oxygen-containing groups will be produced continuously on CNT defects to supplement the consumption of oxygen-containing groups.

However, for catalysts prepared by hydrogen reduction or electrochemical methods, catalyst atoms were deposited on two kinds of CNT sites (step D). Some catalysts were also located at the functional CNT defect sites (site a in step D) and have good electrochemical performance. The others were deposited at CNT perfect sites (site b in step D). The catalysts at CNT perfect sites are facile to be poisoned by poisonous species (mainly CO_{ads}). This depresses the electrochemical performance of catalysts.

Conclusions

An improved DMFC anodic catalyst SR-Pt is prepared from H_2PtCl_6 aqueous solution by functional CNT defects. This process can carry out spontaneously without reducing agent due to the galvanic cell effect between $PtCl_6^{2-}$ ion and functional CNT defects. Catalyst SR-Pt has excellent antipoisoning ability and long-term cycle stability for methanol oxidation, even

superior to PtRu catalysts prepared by hydrogen reduction or electrochemical deposition methods.

Acknowledgment. This work is supported by Program for New Century Excellent Talents in University (NCET-04-0765), Natural Science Foundation of China (50172014), and Scientific Research Foundation for the Returned Overseas Chinese Scholars, State Education Ministry (2001-498).

References and Notes

(1) Löffler, M. S.; Gross, B.; Natter, H.; Hempelmann, R.; Krajewski, T.; Divisek, J. *Phys. Chem. Chem. Phys.* **2001**, *3*, 333.

(2) (a) Löffer, M. S.; Natter, H.; Hempelmann, R.; Wippermann, K. *Electrochim. Acta* **2003**, *48*, 3047. (b) Tripkovic, A. V.; Popovic, K. D.; Grgur, B. N.; Blizanac, B.; Ross, P. N.; Markovic, N. M. *Electrochim. Acta* **2002**, *47*, 3707.

(3) Götz, M.; Wendt, H. *Electrochim. Acta* **1998**, *43*, 3637.

(4) Page T.; Johnson R.; Hormes J.; Noding S.; Rambabu B. *J. Electroanal. Chem.* **2000**, *485*, 34.

(5) (a) Liu, L.; Pu, C.; Viswanathan, R.; Fan, Q. B.; Liu, R. X.; Smotkin, E. S. *Electrochim. Acta* **1998**, *43*, 3657. (b) Chu, Y. H.; Shul, Y. G.; Choi, W. C.; Woo, S. I.; Han, H. S. *J. Power Sources* **2003**, *118*, 334.

(6) Kua, J.; Goddard, W. A., III *J. Am. Chem. Soc.* **1999**, *121*, 10928.

(7) (a) Li, W.; Wang, X.; Chen, Z.; Waje, M.; Yan, Y. *Langmuir* **2005**, *21*, 9386. (b) Waje, M.; Wang, X.; Li, W.; Yan, Y. *Nanotechnology* **2005**, *16*, S395. (c) Wang, X.; Waje, M.; Yan, Y. *Electrochem. Solid-State Lett.* **2005**, *8*, A42. (d) Wang, C.; Waje, M.; Wang, X.; Tang, J. M.; Haddon, R. C.; Yan, Y. *Nano Lett.* **2004**, *4*, 345. (e) Li, W.; Liang, C.; Zhou, W.; Qiu, J.; Zhou, Z.; Sun, G.; Xin, Q. *J. Phys. Chem. B* **2003**, *107*, 6292.

(8) Charlier, J. C. *Acc. Chem. Res.* **2002**, *35*, 1063.

(9) Chen, J.; Hamon, M. A.; Hu, H.; Chen, Y.; Rao, A. M.; Eklund, P. C.; Haddon, R. C. *Science* **1998**, *282*, 95.

(10) Chakrapani, N.; Zhang, Y. M.; Nayak, S. K.; Moore, J. A.; Carroll, D. L.; Choi, Y. Y.; Ajayan, P. M. *J. Phys. Chem. B* **2003**, *107*, 9308.

(11) (a) He, Z. B.; Chen, J. H.; Liu, D. L.; Zhou, H. H.; Kuang, Y. F. *Diam. Relat. Mater.* **2004**, *13*, 1764. (b) Girishkumar, G.; Vinodgopal, K.; Kamat, P. V. *J. Phys. Chem. B* **2004**, *108*, 19960.

(12) Zhang, Y.; Dai, H. J. *Appl. Phys. Lett.* **2000**, *77*, 3015.

(13) (a) Quinn, B. M.; Dekker: C.; Lemay, S. G. *J. Am. Chem. Soc.* **2005**, *127*, 6146. (b) Wang, M. Y.; Chen, J. H.; Fan, Z.; Tang, H.; Deng, G. H.; He, D. L.; Kuang, Y. F. *Carbon* **2004**, *42*, 3257. (c) Tang, H.; Chen, J. H.; Huang, Z. P.; Wang, D. Z.; Ren, Z. F.; Nie, L. H.; Kuang, Y. F.; Yao, S. Z. *Carbon* **2004**, *42*, 191.

(14) Xue, B.; Chen, P.; Hong, Q.; Lin, J. Y.; Tan, K. L. *J. Mater. Chem.* **2001**, *11*, 2378.

(15) (a) Azamian, R.; Coleman, K.; Davis, J.; Hanson, N.; Green, M. *Chem. Commun.* **2002**, *4*, 366. (b) Carrillo, A.; Swartz, J. A.; Gamba, J. M.; Kane, E. S.; Chakrapani, N.; Wei, B.; Ajayan, P. M. *Nano Lett.* **2003**, *3*, 1437.

(16) (a) Liu, Z.; Ling, X. Y.; Su, X.; Lee, J. Y. *J. Phys. Chem. B* **2004**, *108*, 8234. (b) Li, J.; Moskovits, M.; Haslett, T. L. *Chem. Mater.* **1998**, *10*, 1963.

(17) Choi, H. C.; Shim, M.; Bangsaruntip, S.; Dai, H. J. *J. Am. Chem. Soc.* **2002**, *124*, 9058.

(18) Liu, D. Y.; Chen, J. H.; Deng, W.; Zhou, H. H.; Kuang, Y. F. *Mater. Lett.* **2004**, *58*, 2764.

(19) Brankovic, S. R.; McBreen, J.; Adžić, R. R. *J. Electroanal. Chem.* **2001**, *503*, 99.

(20) Yu, R. Q.; Chen, L. W.; Liu, Q. P.; Lin, J. Y.; Tan, K. L.; Ng, S. C.; Chan, H. S. O.; Xu, G. Q.; Andy Hor, T. S. *Chem. Mater.* **1998**, *10*, 718.

(21) Krausa, M.; Vielstich, W. *J. Electroanal. Chem.* **1995**, *399*, 7.

(22) Banerjee, S.; Benny, T. H.; Wong, S. S. *Adv. Mater.* **2005**, *17*, 17.